Preservation of a two-wing Lorenz-like attractor with stable equilibria

L.J. Ontañón-García[a,*], E. Campos-Cantón[b]

[a] Instituto de Investigación en Comunicación Óptica,
[b] Departamento de Físico Matemáticas,
Universidad Autónoma de San Luis Potosí,
Álvaro Obregón 64, 78000,
San Luis Potosí, SLP, México

[b] División de Matemáticas Aplicadas,
Instituto Potosino de Investigación Científica y Tecnológica A.C.
Camino a la Presa San José 2055 col. Lomas 4a Sección, 78216,
San Luis Potosí, SLP, México

Abstract

In this paper, we present the preservation of a two-wing Lorenz-like attractor when in the Lorenz system is applied a feedback control, making two of its equilibria a sink. The forced system is capable of generate bistability and the trajectory settles down at one stable equilibrium point depending on the initial condition when the forced signal is zero. Due to a variation in the coupling strength of the control signal the symmetric equilibria of the Lorenz system move causing the basins of attraction to be dynamic bounded regions that change accordingly. Thus, the preservation of a two-wing Lorenz-like attractor is possible using a switched control law between these dynamic basins of attraction. The forced switched systems also preserve multistabil-

*Corresponding author
Email addresses: luisjavier.ontanon@gmail.com (L.J. Ontañón-García), eric.campos@ipicyt.edu.mx (E. Campos-Cantón)

ity regarding the coupling strength and present multivalued synchronization according to the basin of attraction in which they were initialized. Bifurcations of the controlled system are used to exemplify the different basins generated by the forcing. An illustrative example is given to demonstrate the approach proposed.
Keywords: forced multivalued synchronization, multistability, dynamic basins of attraction.

---

1. Introduction

The idea of having an N-number of equal or different systems by means of sharing a common behavior due to their interaction or by an external signal has been thoroughly studied throughout the years from the point of view of the phenomenon of synchronization. Different ways of synchronization phenomena have been outline, but one of the most remarkable is forced synchronization, where two or more systems are constrained by an external signal. This type of interconnection has unveiled several applications in many scientific areas, as it is in chemistry [1, 2, 3], robotics [4] and geophysics [5], in which an external continuous or periodic signal is received by the forced systems.

About the stability of the forced systems two things are important to considerer after a system is coupled. i) If the forced system looses chaoticity and unpredictability due to the control or suppression of chaos. ii) If the forced system has not only one but multiple regions of stability. Several reports describe methods and applications whereby systems loose some of their intrinsic characteristics in order to adopt inherited properties through

the coupling (see [6, 7] and the references within). Some of these also present multistability, that has been widely used in areas such as medicine [8] and optics [9].

Recently multi-scroll and multi-wing systems have caught attention, and there have been some approaches that present these types of behavior from different techniques, some of them introduce new terms or modify the Lorenz equations [10, 11, 12], some design new systems based on the equilibrium points [13, 14], and some other use different kinds of coupling, such as master-slave system [12] and bidirectional coupling [15].

This work explores forced synchronization phenomenon where the systems are constrained by a feedback control and a perturbation generated by means of a Poincaré plane [16]. This kind of approach allows us to define the shape of a perturbation by a function of time, which is triggered every crossing event of the flow of some monitored system through a previously defined Poincaré plane. Here we have focused on a forced system and its dynamical basins of attraction resulting from a different coupling strength. The highlight of this method lies on three important features:

i) By means of a feedback control and its coupling strength, the Lorenz system presents bistability and becomes stable with two sink equilibria.
ii) The basins of attraction of the system change with respect to a variation in the coupling strength. Taking advantage of these dynamic basins, a switched control law can be designed in order to preserve a two-wing Lorenz-like attractor with stable equilibrium points.
iii) The switched systems present multistablity, and forced multivalued syn-

chronization can be acquired.

The paper is organized as follows: In the Section 2 the multivalued forced synchronization regarding the dynamical basins of attraction is explained; Section 3 presents the characterization of the proposed system; Section 4 contains the forced synchronization method with numerical results; finally, conclusions are drawn in Section 5. Although the perturbation may be any arbitrary signal, here we implement monitoring a system by a Poincaré plane to generate a trigger as an activation of the perturbation, a brief explanation of how to yield this is given in the Appendix A.

2. Multivalued forced synchronization

In order to explain our general approach, let us consider the following identical forced systems:

$$\begin{aligned} \dot{\mathbf{y}}^{\mathbf{1}} &= G(\mathbf{y}^{\mathbf{1}}, \mathbf{u}, \xi), \\ \dot{\mathbf{y}}^{\mathbf{2}} &= G(\mathbf{y}^{\mathbf{2}}, \mathbf{u}, \xi), \\ &\vdots \\ \dot{\mathbf{y}}^{N} &= G(\mathbf{y}^{N}, \mathbf{u}, \xi), \end{aligned} \tag{1}$$

where $2 \leq N \in Z^{+}$ and each $\mathbf{y^i} \in \mathbf{R}^n$, represents the state vector of the forced systems, with corresponding smooth vector field $G : \mathbf{R}^n \times \mathbf{R}^n \times \mathbf{R} \rightarrow \mathbf{R}^n$, $\mathbf{u} \in \mathbf{R}^n$ and $\xi \in \mathbf{R}$ stand for the control signal and a perturbation, respectively.

The function G in Eq. (1) includes all terms on dynamics, coupling and perturbation. It can be rewritten in the following form, $G(\mathbf{y}, \mathbf{u}, \xi) = G_a(\mathbf{y}) + \mathbf{B}\mathbf{u}(t) + \mathbf{C}\xi(t)$ (see [17]), where G_a stands for the dynamics of the

autonomous system, *i. e.*, before being forced and $\mathbf{B} \in \mathbf{R}^{n\times n}$ determines which states are feedback, the control signal $u := KG_c$ is conformed by $G_c : \mathbf{R}^n \to \mathbf{R}^n$ function of the state vector of the system which acts as a feedback and $K \in \mathbf{R}$ is the strength of the dissipative coupling. $\mathbf{C} \in \mathbf{R}^n$ determines which states are perturbed.

To detect stability and synchronization in the proposed method we use the Maximum Conditional Lyapunov Exponent (MCLE) [18, 19]. Worth mentioning that the MCLE is always negative when the forced system is synchronized but it cannot detect a multivalued synchronization. Thus we decided to measure the distance between the trajectories of two forced systems with different initial conditions in order to detect a different basin of attraction.

In order to define the multivalued forced synchronization, we assume the constrained systems given by Eq. (1) induce in phase space $\mathbf{R}^n$ the flow $(\varphi^t), t \in \mathbf{R}$ such that each forward trajectory of the initial point $\mathbf{y}_0^i$ is the set $\{\mathbf{y}^i(t) = \varphi^t(\mathbf{y}_0^i, K, \xi) : t \geq 0\}$. We assume the forced systems given by Eq. (1) have a dissipative bounded region $\mathcal{D} \subset \mathbf{R}^n$, such that the flow $\varphi^t(\mathcal{D}, K, \xi) \subset \mathcal{D}$ for every $t \geq 0$. The maximal attractor $\mathcal{A}$ is the largest attracting invariant subset of $\mathcal{D}$.

Remark 2.1. *Throughout this work, reference is made to the flow as a set of two or more trajectories.*

The notion of multivalued forced synchronization takes place for multiple modes in the synchronization regime and can be defined as follows:

Synchronization in a multivalued mode: Let $\mathbf{u} \in \mathbf{R}^n$ be a control vector, ξ be a perturbation and $\mathbf{y}_0^1, \mathbf{y}_0^2, \ldots, \mathbf{y}_0^N \in \mathbf{R}^n$ be initial conditions

$\mathbf{y}_0^i = \mathbf{y}^i(t=0)$ for the N forced systems given by Eq. (1) with $\mathbf{y}_0^i \neq \mathbf{y}_0^j$ for $i \neq j$. Then the forced systems are said to be synchronized at $\mathbf{y}_0 = (\mathbf{y}_0^i, \mathbf{y}_0^j)$ in a multivalued mode if there exists open sets $V_i \ni \mathbf{y}_0^i$ in $\mathcal{D}$ such that for every $\mathbf{y}_0^j \in V_j \subset \mathcal{D}$ the trajectories $\varphi^t(\mathbf{y}_0, K, \xi) = (\mathbf{y}^i(t), \mathbf{y}^j(t))$ satisfies the asymptotic condition if $V_i = V_j$. However the forced systems do not identical synchronize if $\varphi^t(\mathbf{y}_0, K, \xi)$ belongs to different basin of attraction $V_i \neq V_j$

$$\lim_{t\to\infty} |\mathbf{y}^i(t) - \mathbf{y}^j(t)| = \begin{cases} 0, & \text{for } V_i = V_j; \\ d_{ij} > 0, & \text{for } V_i \neq V_j. \end{cases} \tag{2}$$

where d_{ij} is an arbitrary distance.

Remark 2.2. *Since the forced systems are identical then the dissipative bounded region $\mathcal{D}$ is the same for all systems. Inasmuch as $\mathcal{D}$ can be made up by several open sets V_i then forced systems converge to one open set V_i depending on a particular initial condition $\mathbf{y}_0^j, j = 1, ..., N$*

The aforementioned definition assumes that if the system from Eq. (1) is in a multivalued forced synchronization regime with multiplicity p, then there are p open sets V_i, $i = 1, ..., p$. Thus, for a given control signal u and perturbation ξ, the distance $|\mathbf{y}^i(t) - \mathbf{y}^j(t)|$ has p different asymptotic behaviors, depending on the initial conditions $\mathbf{y}_0^i \in V_i(\mathbf{y}_0)$ and $\mathbf{y}_0^j \in V_j(\mathbf{y}_0)$ of the forced systems.

This is because of multivalued mode of synchronization regime, the dissipative bounded region $\mathcal{D}$ is the union of disjointed open sets. That is, for a given initial point $(\mathbf{y}_1) \in \mathcal{D}$ let us denote $V_1(K) \ni \mathbf{y}_1$ as its largest neighborhood of multivalued synchronization in $\mathcal{D}$. Assume that the set $\mathcal{D} - V_1(K)$ is not empty. Then, $V_2(K)$ is the largest neighborhood of multivalued synchronization for an initial condition $\mathbf{y}_2 \in V_2(K) \subset \mathcal{D} - \overline{V_1(K)}$. Similarly, a

neighborhood of multivalued synchronization $V_3(K)$ is defined for an initial condition $\mathbf{y}_3 \in V_3(K) \subset \mathcal{D} - (\overline{V_1(K)} \bigcup \overline{V_2(K)})$, and so on, up to a $V_p(K)$, $p \geq 2$.

3. Stability in the forced Lorenz systems

The Lorenz system is given by:

$$\begin{aligned} \dot{y}_1 &= \sigma(y_2 - y_1), \\ \dot{y}_2 &= \rho y_1 - y_2 - y_1 y_3, \\ \dot{y}_3 &= y_1 y_2 - \beta y_3, \end{aligned} \tag{3}$$

where y_1, y_2 and y_3 are the states, and the parameters $\sigma = 10$, $\rho = 25$ and $\beta = 8/3$, locate the system in a chaotic regime.

The feedback function of the state vector will take the form $G_c = (y_1, 0, 0)^T$, and only one state will be forced so

$$\mathbf{B} = \begin{pmatrix} -1 & 0 & 0 \\ 0 & 0 & 0 \\ 0 & 0 & 0 \end{pmatrix} \text{ and } \mathbf{u} = (K y_1, 0, 0)^T.$$

Considering a perturbation on the state y_1, then $\mathbf{C} = (1, 0, 0)^T$. Summarizing the forced systems results as follows:

$$\dot{\mathbf{y}}^{\mathbf{i}} = \begin{bmatrix} \dot{y}_1 \\ \dot{y}_2 \\ \dot{y}_3 \end{bmatrix} + \begin{bmatrix} -K y_1 \\ 0 \\ 0 \end{bmatrix} + \begin{bmatrix} \xi \\ 0 \\ 0 \end{bmatrix}, \tag{4}$$

where $i = 1, 2, \ldots, N$ stands for the number of coupled systems.

Considering $\xi = 0$ and $N = 1$ in order to study the stability of the equilibria as a function of the K coupling strength. The equilibria of the coupled system is given by:

$$Q = (\quad 0, \quad 0, \quad 0 \quad), \tag{5}$$

$$R = (\quad \eta, \quad \eta\mu, \quad \rho - \mu \quad), \tag{6}$$

$$S = (\quad -\eta, \ -\eta\mu, \ \rho - \mu \quad), \tag{7}$$

where $\eta = \sqrt{\beta\left(\frac{\sigma\rho}{\sigma+K} - 1\right)}$ and $\mu = \frac{(\sigma+K)}{\sigma}$. Notice that the Q equilibrium point is independent of the values of parameters and the coupling force, in contrast to the R and S equilibrium points that vanish when $\sigma\rho < (\sigma + K)$. Since R and S given by Eqs. (6) and (7) depend on the coupling strength, we present the location of these equilibrium points for a variation of $0 \leq K \leq 240$ in Figure 1, where the Q equilibrium point is marked with asterisk remains at the origin for any value of K, however, the other two points marked with diamonds for R and circles for S begin to approach to the origin as K tends to increase.

The local stability of the equilibrium points also depend on the coupling strength. The eigenvalues for the equilibria Q, R and S given by the Jacobian of system (4) for $\xi = 0$ can be appreciated in Figure 2. Here we depicted their values for the same variation of $0 \leq K \leq 240$. Figure 2 a) shows the eigenvalues corresponding to Q which are all real, the positive one begins to approach zero as K increases. The equilibrium points R and S have the same stability, which are shown in Figure 2 b). Each of these two points presents a saddle equilibrium point for $K < 0.1$, *i. e.*, two of their eigenvalues are complex conjugate with positive real part and the other is real negative.

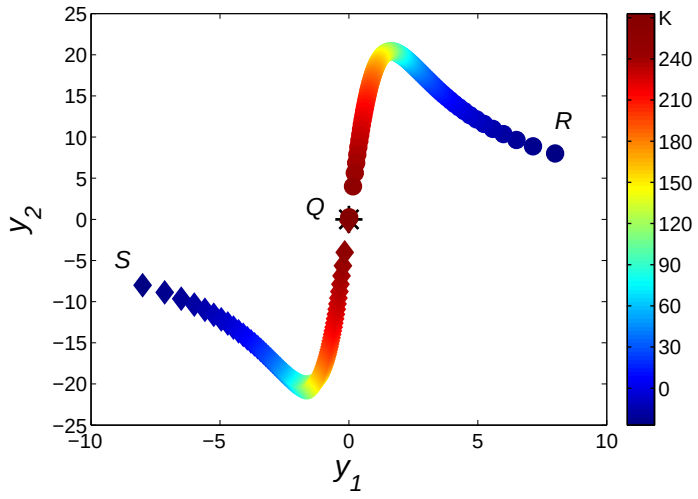

Figure 1: Location of the equilibrium points of system (4) projected onto the (y_1, y_2) plane. These points were calculated due to a variation on the coupling strength for $0 \leq K \leq 240$ depicted with the colors of the bar in the right. The three points are marked with asterisks for Q from Eq. (5), circles and diamonds for R from Eq. (6) and S from Eq. (7), respectively.

In the interval of $0.1 < K < 170$, the saddle disappears due to the complex conjugate real parts changes from positive to negative. For values of $K > 170$ all the eigenvalues turn negative real meaning that both equilibrium points become sink, and any trajectory near them will be attracted to them. This is the reason why the phenomena of bistability occurs for $0.1 < K < 240$, notice that trajectories converge to an equilibrium point depending on the initial condition given to each forced system and the basin of attraction that it corresponds.

4. Multistability by forced Lorenz systems

The perturbed signal ξ can be generated in many ways as previously discuss. We will focus on the generation of the perturbed signal in the same spirit as in [16], only considering the viewpoint of activation. A brief explanation is described in Appendix A, and ξ will take the form $\xi = Ae^{-\tau(t-t_i)}\cos(w(t-t_i))$ from Eq. (A.2) taken from a Rössler system as in [16], where A increases accordingly K increases, we particularly considered $A = K$. Here $0 \leq \tau \in \mathbf{R}$ represents an underdamping factor which allows us to modulate the signal and the scalar $w \in \mathbf{R}$ stands for the frequency. Thereby is possible to generate a process akin to a Poisson process, but instead of be a stochastic process is chaotic.

Figure 3 a) shows a projection of the forced system onto the (y_1, y_2) plane

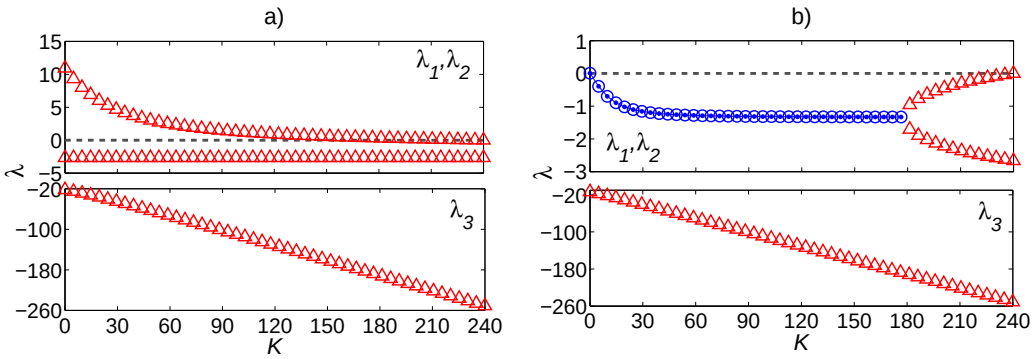

Figure 2: Jacobian eigenvalues of the equilibrium points of the forced system due to a variation of the coupling strength for $0 \leq K \leq 240$. The eigenvalue was marked with red triangle when is a real value and with blue circle or dot when is complex, in the upper graphic λ_1, λ_2 and in the lower graphic λ_3. a) Eigenvalues corresponding to the equilibrium point at origin. b) Eigenvalues corresponding to symmetrical equilibrium points given by (6) and (7).

for $K = 20$. The size of the attractor is tiny because the system is stable and every initial condition goes to the equilibrium point, but the perturbation makes the system's trajectory to oscillate around the stable equilibrium points. Figure 3 b) shows the MCLE of the system for different values of the coupling strength, the range vary from $0 \leq K \leq 240$. For values of K greater than 4 the system presents a negative Lyapunov exponent, meaning that the forced systems can be synchronized in presence of the same perturbations. However with the MCLE is not possible to know whether the trajectories are in the same basin of attraction or a different one. In order to detect the multistability in the coupled system we calculated the Euclidean distance between the trajectories of two forced systems with different initial conditions.

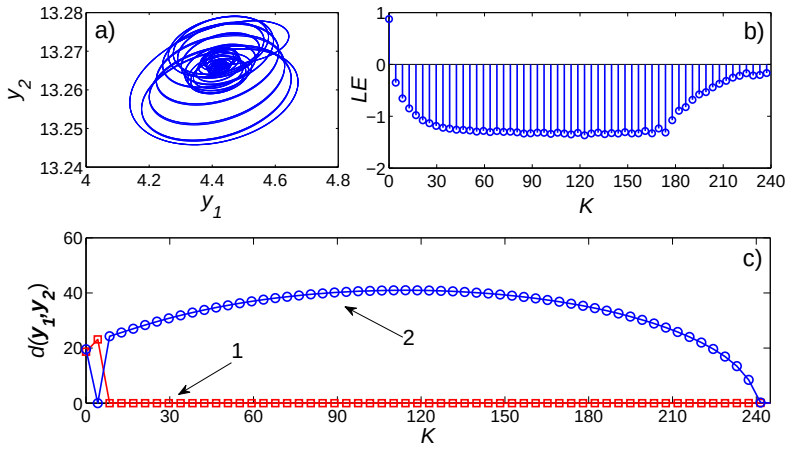

Figure 3: a) Projection of the system Eq. (4) in the (y_1, y_2) plane for $K = 20$, $\tau = 1/1000$, $\omega = \pi/50$. b) Maximum Conditional Lyapunov Exponent due to a variation in the coupling strength $0 \leq K \leq 240$. c) Euclidean distance between the trajectories of forced systems with different sets of initial conditions. For the line "1" marked with squares $(\mathbf{y}_0^1,\ \mathbf{y}_0^2)$. For the line "2" marked with circles $(\mathbf{y}_0^1,\ \mathbf{y}_0^3)$.

This distance was calculated from $d(\mathbf{y}^1, \mathbf{y}^2) = \sqrt{\sum_{i=1}^{n}(\mathbf{y}^1[i] - \mathbf{y}^2[i])^2}$, where n stands for the number of iterations in the numerical simulation made with a fourth-order Runge Kutta method, for this case we considered $n = 100,000$ iterations after the transient state.

The sets of initial conditions considered are given by:

$$\mathbf{y}_0^1 = (1,\ 1,\ 1), \tag{8}$$

$$\mathbf{y}_0^2 = (7,\ 8,\ 24), \tag{9}$$

$$\mathbf{y}_0^3 = (-7, -8, -24). \tag{10}$$

Notice in Figure 3 c) from line 1 marked with squares that there is complete synchronization at $(\mathbf{y}_0^1, \mathbf{y}_0^2)$ and the asymptotic condition Eq. (2) is met due to $\mathbf{y}_0^1$ and $\mathbf{y}_0^2$ belong to the same open set V_1 for $10 < K < 240$. The set $\mathbf{y}_0^1$ and $\mathbf{y}_0^3$, results on different behaviors between the forced systems, this is shown in Figure 3 c) from the line 2 marked with circles. The forced systems present generalized synchronization at $(\mathbf{y}_0^1, \mathbf{y}_0^3)$ and the trajectory $\varphi^t(\mathbf{y}_0^1, \mathbf{y}_0^3)$ does not satisfy the asymptotic condition due to $d(\mathbf{y}^1, \mathbf{y}^3) > 0$, so $\mathbf{y}_0^1 \in V_1$ and $\mathbf{y}_0^3 \in V_2$ with $V_1 \neq V_2$ for $10 < K < 240$. The trajectories oscillate near the equilibrium points R and S for the two different basins of attraction. Figure 4 shows a bifurcation diagram calculated by means of local maxima of the time series y_1 when the forced systems present bistability, $4 \leq K \leq 240$. The upper branch of Figure 4 shows when the trajectory oscillates around the S equilibrium point and the below branch shows oscillation around the R equilibrium point.

In this systems configuration, only two basins of attraction emerge. These

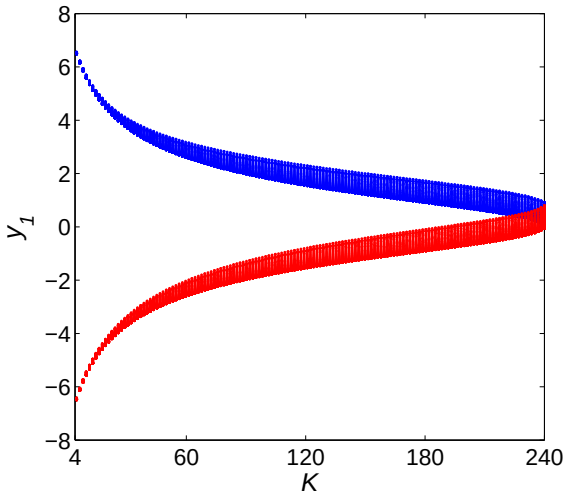

Figure 4: Bifurcation diagram of the forced Lorenz system in the y_1 state for different values of the coupling strength K. The trajectories in the two different basins of attraction are marked with blue and red.

two basins may be appreciated in Figure 5, where the $y_3 = 4$ plane for the region $-50 \leq y_1 \leq 50$ and $-50 \leq y_2 \leq 50$ are shown for different values of the coupling strength K. Figure 5 a) shows the two different basins for $K = 5$, calculated with the Euclidean distance, one is marked with red circles and the other one with blue dots. These two basins of attraction are interlaced, presenting irregular forms. However in Figure 5 b) for $K = 200$, the basins are dividing the grid, but the irregular structure has been lost. This is a clear example of how the basins of attraction are being dynamic respect to the value of K.

Remark 4.1. *When there are multiple basins of attraction where synchronization occurs, the dissipative bounded region $\mathcal{D}$ is the union of disjointed open sets that are localized in different parts of $\mathbf{R}^n$.*

With the forcing signal the Lorenz-type oscillations are lost, instead they occur near the equilibrium point in the corresponding basin of attraction.

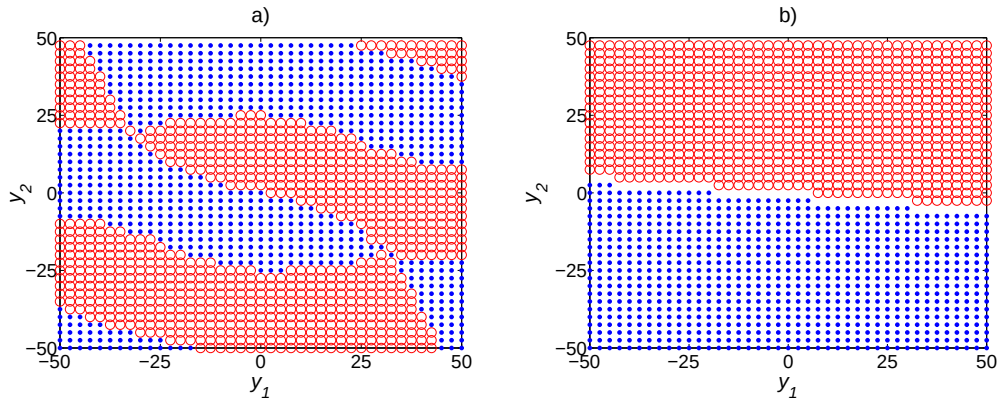

Figure 5: Two basins of attraction on the $y_3 = 4$ plane for the region $-50 \leq y_1 \leq 50$ and $-50 \leq y_2 \leq 50$ for different values of the coupling strength: a) $K = 5$, b) $K = 200$. The basins V_1 and V_2 are marked with red circles and blue dots, respectively.

Two-wing Lorenz-like attractor

Due to the dynamic basins of attraction V_1 and V_2 as a function of the coupling parameter K, we are able to design a switched system with specific values of the coupling strength $K_1, K_2, \ldots, K_n$ that determine a pair of equilibrium points R_1, S_1, R_2, S_2, $\ldots$, R_n, S_n that belong to basins of attraction $V_{1,2}(K_1), V_{1,2}(K_2), \ldots, V_{1,2}(K_n)$, respectively. With the purpose of describing the switched system, let us define a neighborhood around a given point $\mathbf{x} \in \mathbf{R}^3$ as $N_\delta(\mathbf{x}) = \{\mathbf{y} \in R^3 | d(\mathbf{x}, \mathbf{y}) < \delta\}$, where δ is a scalar that stands for the radius of each $N_\delta(\mathbf{x})$ neighborhood.

Suppose that $R_1 \in V_1(K_1), S_1 \in V_2(K_1), R_2 \in V_1(K_2), S_2 \in V_2(K_2), ..., R_n \in V_1(K_n), S_n \in V_2(K_n)$. Now the idea is to initialize a forced system with $\mathbf{y}_{01} \in \mathcal{D}$ and a specific value for the coupling strength K_1, when the forward

trajectory $\varphi(\mathbf{y}_{01}, K_1, \xi)$ of the initial condition enters to whatever neighborhood $N_\delta(R_1)$ or $N_\delta(S_1)$, the coupling strength will be changed to K_2 and at this time the system will be initialized with the current location of the trajectory $\mathbf{y}_{02} = \varphi(\mathbf{y}_{01}, K_1, \xi)$. Hence the new forward trajectory $\varphi(\mathbf{y}_{02}, K_2, \xi)$ changes the value of coupling strength to K_3 until it enters to any neighborhood $N_\delta(R_2)$ or $N_\delta(S_2)$, and so on. The coupling strength will return to its starting value K_1 when the trajectory $\varphi(\mathbf{y}_{0n}, K_n, \xi)$ enters to any neighborhood $N_\delta(R_n)$ or $N_\delta(S_n)$ and the cycle begins again.

For each time the system switches the coupling strength, the basins of attraction also switch depending on the value of K. For specific values of the coupling strength and taking into consideration the interlacing of the resulting basins and initial conditions, it is possible to preserve a two-wing Lorenz-like attractor with stable equilibrium points.

In order to explain this in more detail we will start by considering one forced system from Eq. (4) with a perturbation ξ given by Eq. (A.2). Without loss of generality, the approach is exemplified by taking two values for $K_{1,2} = 5, 200$. These coupling strengths $K_1 = 5$ and $K_2 = 200$ determine the location of the pairs of equilibrium points at $S_1 = (-6.45,\ -9.7,\ 23.5)$ and $R_1 = (6.45,\ 9.7,\ 23.5)$, and $S_2 = (-0.73,\ -14.94,\ 4)$ and $R_2 = (0.73,\ 14.94,\ 4)$, respectively. Now, considering the following initial conditions $x_{01} = (0.73,\ 14.94,\ 4) \in V_1(K_1)$ and $x_{02} = (-0.73,\ -14.94,\ 4) \in V_2(K_1)$ that correspond to the location of the equilibrium points R_2 and S_2 determined by $K_2 = 200$, respectively. The forward trajectories $\varphi(x_{01} = R_2, K_1, \xi) \in V_1(K_1) \to S_1$ and $\varphi(x_{02} = S_2, K_1, \xi) \in V_2(K_1) \to R_1$ will be led to oscillate near the equilibrium points. This is depicted in Figure 6 a),

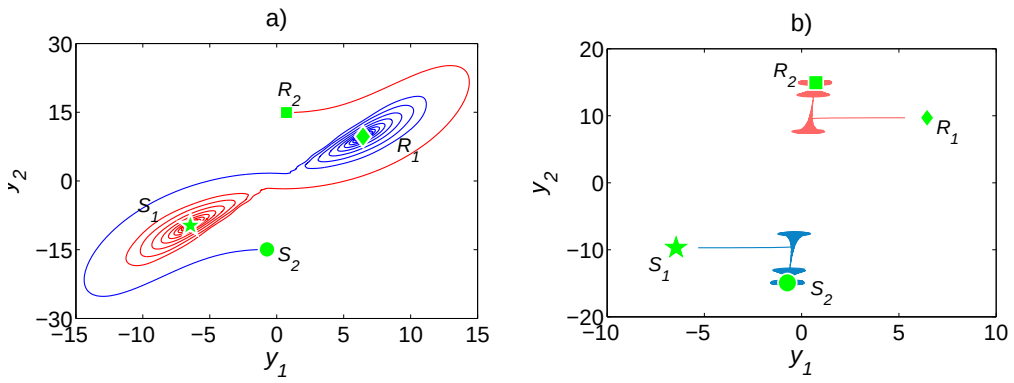

Figure 6: Projection onto the (y_1, y_2) plane for two different sets of initial conditions marked with green dots and different values of the coupling strength. The two resulting trajectories are marked with red and blue. a) The initial conditions are $x_{01} = R_2 = (0.73,\ 14.94,\ 4)$, and $x_{02} = S_2 = (-0.73,\ -14.94,\ 4)$, with $K_1 = 5$. b) The initial conditions are $x_{03} = R_1 = (6.45,\ 9.7,\ 23.5)$, and $x_{04} = S_1 = (-6.45,\ -9.7,\ 23.5)$, with $K_2 = 200$.

where both forward trajectories are marked with blue and red, respectively, the initial condition $x_{01} = R_2$ is marked with a green square and $x_{02} = S_2$ with a green circle. The equilibrium points $R_1 \in V_2(K_1)$ and $S_1 \in V_1(K_1)$ are marked with a green diamond and a green star, respectively.

Now by changing the coupling strength to $K_2 = 200$ and selecting the set of initial conditions at $x_{03} = R_1 = (6.45,\ 9.7,\ 23.5)$ and $x_{04} = S_1 = (-6.45,\ -9.7,\ 23.5)$, the trajectories of the systems converge to each corresponding basin of attraction $V_1(K_2)$ and $V_2(K_2)$, respectively. This may be appreciated in Figure 6 b), where the two systems trajectories are marked with blue and red, also the set of initial conditions $x_{03} = R_1 \in V_1(K_2)$ and $x_{04} = S_1 \in V_2(K_2)$ are marked as a green diamond and a green star, respectively, and the equilibrium points S_2 in a green circle and R_2 as a green

square, respectively.

Notice that the equilibrium points R_1 and S_1 for K_1 correspond to the initial conditions x_{03} and x_{04}, respectively, and the equilibrium points R_2 and S_2 for K_2 correspond to the initial conditions x_{01} and x_{02}, respectively.

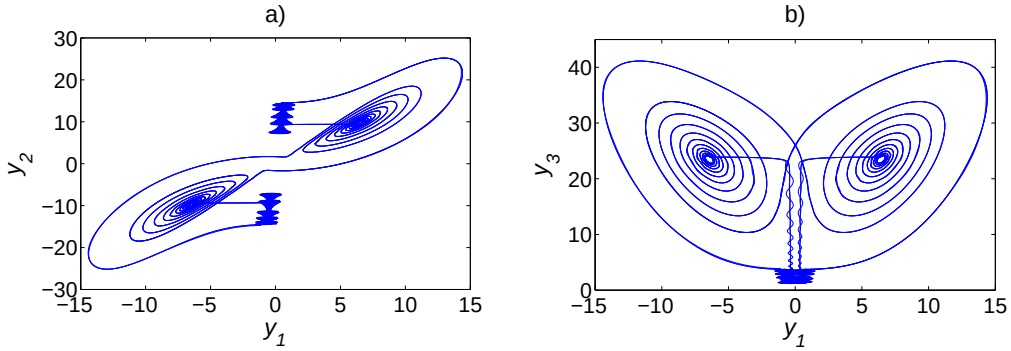

Figure 7: Preservation of a two-wing Lorenz-like attractor from the switched law in Eq. (11) for $K_1 = 5$, $K_2 = 200$ and $\delta = 0.05$. a) Projection onto the (y_1, y_2) plane. b) Projection onto the (y_1, y_3) plane.

Focusing on this resulting basins and in the interconnection with the initial conditions due to the coupling strength, we choose the neighborhoods $N_\delta(R_1), N_\delta(S_1), N_\delta(R_2), N_\delta(S_2)$ with $\delta = 0.05$. Then we may define the switched system given by Eq. (4) and starting with $K = K_1$ and changing as follows:

$$K = \begin{cases} K_1 & \mathbf{y}(t) \in N_\delta(R_2) \text{ or } \mathbf{y}(t) \in N_\delta(S_2); \\ K_2 & \mathbf{y}(t) \in N_\delta(R_1) \text{ or } \mathbf{y}(t) \in N_\delta(S_1). \end{cases} \tag{11}$$

Figure 7 a) shows a projection onto the (y_1, y_2) plane of the resulting attractor of the switched system. Here we can see the similarity with the oscillations for the independent values of the coupling strengths K_1 and K_2 depicted in Figure 6 a) and b). The two-wing structure can be appreciated

in more detail from the projection onto the (y_1, y_3) plane depicted in Figure 7 b), and the dynamics of each independent state may be seen in Figure 8 a) the time series of the y_1 state, b) y_2 state and c) y_3 state.

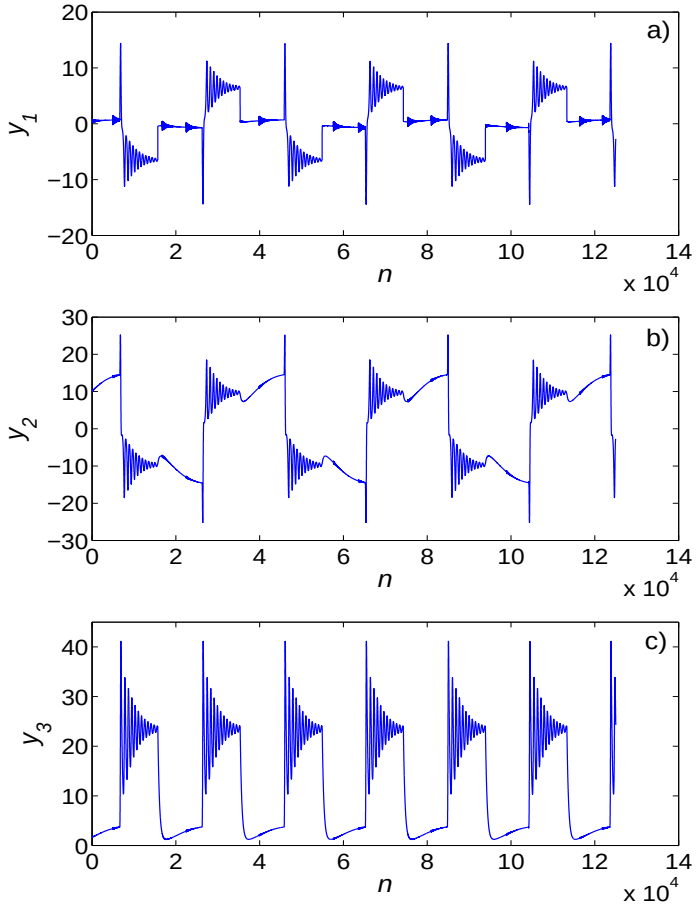

Figure 8: Time series of the states of the resulting two-wing Lorenz-like attractor with $K_1 = 5$ and $K_2 = 200$ for some iterations in time: a) y_1, b) y_2, c) y_3.

Generalized synchronization via forced switched systems

Since the switched systems are being forced by the same perturbation, this subsection is devoted to study synchronization among them. So we

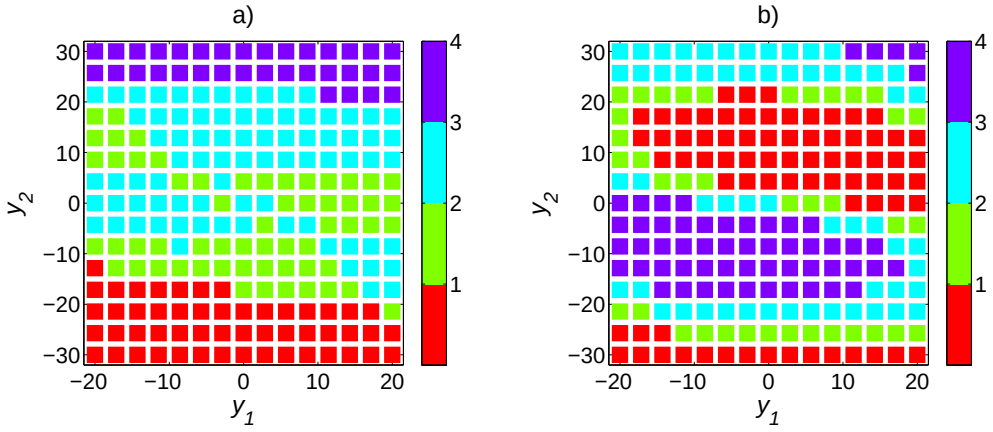

Figure 9: Four basins of attraction of the forced switched system in the a) $y_3 = 4$ plane, b) $y_3 = 24$ plane for the region $-20 \leq y_1 \leq 20$ and $-30 \leq y_2 \leq 30$.

initialized two of them with different initial conditions. By controlling two forced systems with the switched control law given by Eq. (11), with $K_1 = 5, K_2 = 200$ and using two different sets of initial conditions we can detect the region where the basins of attraction are located using the Euclidean distance between the forced systems. The result is that after the switching of the coupling strength, the systems present four basins instead of two as the regular system does for one value of the coupling strength.

The location of these different basins of attraction can be seen in Figure 9, for different regions on planes perpendicular to y_3 axis. Figure 9 a) shows the $y_3 = 4$ plane and Figure 9 b) the $y_3 = 24$ plane for the region $-20 \leq y_1 \leq 20$ and $-30 \leq y_2 \leq 30$.

Remark 4.2. *For* $\mathcal{A} \subset \overline{\bigcup_{i=1}^{p} V_i(K)}$, $\mathbf{y}(t) = \varphi^t(\mathbf{y}_0, K, \xi)$ *goes through each* $V_i(K)$ *an infinite number of times for every* $\mathbf{y}_0 \in \mathcal{D}$. *The basins of attraction where synchronization occurs are not static sets. For each initial condition* $\mathbf{y}_0 \in \mathcal{A}$ *the time evolution of the basin of attraction* $V_i(K)$ *is denoted by*

$V^t(K) := \varphi^t(\mathbf{y}_0, K, \xi)$.

As aforementioned, the four basins exist, and the systems synchronize and satisfy the asymptotic condition from Eq. (2). In addition of preserving the two-wing Lorenz-like attractor, the coupled systems preserve multistability in their phase space due to the switching of the coupling strength and they are capable of synchronize regarding of whether the initial conditions belong to the same basin of attraction or not. Different switched control law's including a large number of coupling strengths may be designed in order to have more complex attractors.

5. Concluding remarks

Multistability is presented in the Lorenz system by applying a perturbation and a feedback control law. The perturbation signal ξ may be periodic, random or chaotic as some existing system in nature (see [20]). Here it was generated by means of a monitored chaotic system by a Poincaré plane in order to avoid periodicity and simulate a perturbation similar to a Poisson process. The variation in the coupling strength K changes the stability of the forced system and modifies the region of the corresponding basins of attraction. The different basins of attraction are detected by checking the asymptotic behavior of different initial conditions, depicted by means of the bifurcation diagram and the projection of the equilibrium points for different values of K. Taking advantage of the dynamics of the basins of attractions of the stable system the flow of the trajectory may be redirected preserving a two-wing Lorenz-like attractor.

The forced synchronization has application in chaotic communication systems, where there are always at least two forced systems involved: i) the transmitter, which has the information signal as its external driving and ii) the receiver, which is forced by the incoming carrier delivered by the transmitter. The goal of a communication systems is achieved when the transmitter forces the receiver to synchronize. Thus the forced synchronization in a Lorenz-like system can be used to construct a communication system and the key to synchronize due to the multivalued synchronization is the sequence that the coupled strength can take. This work is under investigation and may be reported elsewhere.

Acknowledgments

L.J.O.G. is a doctoral fellow of CONACYT in the Graduate Program on Applied Science at IICO-UASLP. E.C.C. acknowledges CONACYT for the financial support through project No. 181002.

References

[1] M.E.E. Abashar and S.S.E.H. Elnashaie, Multistablity, bistability and bubbles phenomena in a periodically forced ethanol fermentor, Chemical Engineering Science vol. **66**, pp. 6146–6158 (2011).

[2] M.E.E. Abashar, Dynamic phenomena in forced bioethanol reactors, Computers and Chemical Engineering vol. **37**, pp. 172–183, (2012).

[3] M.F. Perez-Polo and M. Perez-Molina, Self-oscillating chaotic behavior and induced oscillations of a continuous stirred tank reactor with

nonlinear control, Chemical Engineering Journal vol. **191**, pp. 512–527, (2012).

[4] Z.G. Zhang, H. Kimura. and K. Takase, Adaptive running of a quadruped robot using forced vibration and synchronization, Journal of Vibration and Control, vol. **12**, pp. 1361–1385, (2006).

[5] F.J.R. Eccles, P.L. Read, and T.W.N. Haine, Synchronization and chaos control in a periodically forced quasi-geostrophic two-layer model of baroclinic instability, Nonlinear Processes in Geophysics vol. **13**, pp. 23–39, (2006).

[6] S. Boccaletti, C. Grebogi, Y.C. Lai, H. Mancini and D. Maza, The control of chaos: Theory and applications, Physics Reports vol. **329**, pp. 103–197 (2000).

[7] B. R. Andrievskii and A. L. Fradkov, Control of chaos: Methods and applications. II. Applications, Automation and Remote Control, vol. **65**, No. 4, pp. 505–533, (2004).

[8] J. Milton and P. Jung, Epilepsy as a dynamic disease, New York: Springer-Verlag, (2002).

[9] F. T. Arecchi, R. Meucci, G. Puccioni and J. Tredicce, Experimental evidence of eubharmonic bifurcations, multistability and turbulence in a Q-switched gas laser, Phys. Rev. Lett., vol. **49**, pp. 1217–1220, (1982).

[10] G. Qi, G. Chen, M.A. van Wyk, B.J. van Wyk and Y. Zhang, A four-wing chaotic attractor generated from a new 3-D quadratic autonomous system, Chaos, Solitons and Fractals vol. **38**, pp. 705–721, (2008).

[11] S. Yu, W.K.S. Tang, J. Lü and G. Chen, Multi-wingbutterfly attractors from the modified Lorenz systems, Circuits and Systems. ISCAS 2008. IEEE International Symposium, pp. 768–771, (2008).

[12] K. Bouallegue, A. Chaari and A. Toumi, Multi-scroll and multi-wing chaotic attractor generated with Julia process fractal, Chaos, Solitons and Fractals vol. **44**, pp. 79–85, (2011).

[13] S. Cang, G. Qi and Z. Chen, A four-wing hyper-chaotic attractor and transient chaos generated from a new 4-D quadratic autonomous system, Nonlinear Dyn. vol. **59**, pp. 515–527, (2010).

[14] S. Dadras, H.R. Momeni, G. Qi and Z.L. Wang, Four-wing hyperchaotic attractor generated from a new 4D system with one equilibrium and its fractional-order form, Nonlinear Dyn vol. **67**, pp. 1161–1173, (2012).

[15] G. Grassi, F.L. Severance and D.A. Miller, Multi-wing hyperchaotic attractors from coupled Lorenz systems, Chaos, Solitons and Fractals vol. **41**, pp. 284–291, (2009).

[16] L.J. Ontañón-García, E. Campos-Cantón, R. Femat, I. Campos-Cantón and M. Bonilla-Marín, Multivalued synchronization by Poincaré coupling, Commun. Nonlinear Sci. Numer. Simulat., http://dx.doi.org/10.1016/j.cnsns.2013.02.015.

[17] N.F. Rulkov, M.M. Sushchik, L.S. Tsimring and H.D.I. Abarbanel, Generalized synchronization of chaos in directionally coupled chaotic systems, Phys. Rev. E vol. **51**, pp. 980–994, (1995).

[18] L.M. Pecora, T.L. Caroll, G.A. Johnson, D.J. Mar and J. F. Heagy, Fundamentals of synchronization in chaotic systems, concepts, and applications, Chaos 7**4**, (1997).

[19] L.M. Pecora and T.L. Caroll, Driving systems with chaotic signals, Phys. Rev. A vol. **44**, (1991).

[20] L.J. Ontañón-García, E. Campos-Cantón, Discrete coupling and synchronization in the insulin release in the mathematical model of the β cells, Discrete dynamics in nature and society, (2013), doi 10.1155/2013/427050.

[21] J. Lü, T. Zhou, G. Chen and S. Zhang, Local Bifurcations of the Chen System, Int. J. Bif. Chaos, vol. **12**, pp. 2257–2270, (2002).

Appendix A. Perturbed Signal

Although the perturbation ξ can be generated in several ways, usually is considered as a periodical signal, but in order to avoid the periodicity we take the model of triggering given by [16]. An autonomous system described as:

$$\mathbf{x}' = \quad F(\mathbf{x}), \quad F : \mathbf{R}^m \to \mathbf{R}^m \tag{A.1}$$

is being monitored by a Poincaré plane $\Sigma := \{(\mathbf{x}_1, \mathbf{x}_2, \mathbf{x}_3) : \alpha_1\mathbf{x}_1 + \alpha_2\mathbf{x}_2 + \alpha_3\mathbf{x}_3 + \alpha_4 = 0\}$ where $\alpha_1, \ldots, \alpha_4 \in \mathbf{R}$ are coefficients of a hyperplane equation whose values are considered arbitrarily according to the following discussion. We are interested in the crossing events of the trajectory of the monitored

system Eq. (A.1) restricted to the projection $\mathcal{A}_x$ with Σ, captured by the points $\{\varphi_m^{t_0}(\mathbf{x}_0), \varphi_m^{t_1}(\mathbf{x}_0), \varphi_m^{t_2}(\mathbf{x}_0), \ldots\} \in \Sigma$ at each crossing event. Where $\varphi_m^{t_i}(\mathbf{x}_0)$ is the flow restricted to $\mathcal{A}_x$. Therefore, we can specify the following time series $\Delta_{\mathbf{x}_0} = \{t_0, t_1, t_2, \ldots\}$, which depends on the initial conditions of the system in Eq. (A.1). The location of the plane must be located in order to meet the condition $\mathcal{A}_x \bigcap \Sigma \neq \emptyset$, assuming that at least one crossing event at time t_i exists. Throughout this work we have focused in the crossing events of the trajectory of the monitored system with Σ in only one direction. So the time series $\Delta_{\mathbf{x}_0}$ contains each crossing event that satisfy $\frac{d}{dt}(x_1) > 0$. Following the above discussion, the term $\xi(t)$ from equation (1) is determined as follows:

$$\xi(t) = (Ae^{-\tau(t-t_i)}\cos(w(t-t_i)), 0, 0)^T, \tag{A.2}$$

where $\tau \in \mathbf{R}$ represents an underdamping factor which allows us to modulate the signal and the scalar $w \in \mathbf{R}$ stands for the frequency. Therefore the underdamped signal is triggered with each crossing event of Eq. (A.1) with Σ. Notice that for a value of $\tau = 0$, the coupling becomes the negative feedback from the classical form described above [17]. Figure A.10 a) shows the projection of the Chen system [21] with the following equations:

$$\begin{aligned} \dot{x}_1 &= a(x_2 - x_1), \\ \dot{x}_2 &= (c-a)x_1 - x_1x_3 + cx_2, \\ \dot{x}_3 &= x_1(x_2 - bx_3). \end{aligned} \tag{A.3}$$

with the parameters $a = 35, b = 3, c = 28$. The system is being monitored by a Poincaré plane with values $\alpha_1 = 0.5934, \alpha_2 = -1.1636, \alpha_3 = 0, \alpha_4 =$

-2.4068, every event of crossing between the system and the plane Σ is marked with an asterisk. And the form of the signal (A.2) generated is depicted in Figure A.10 b).

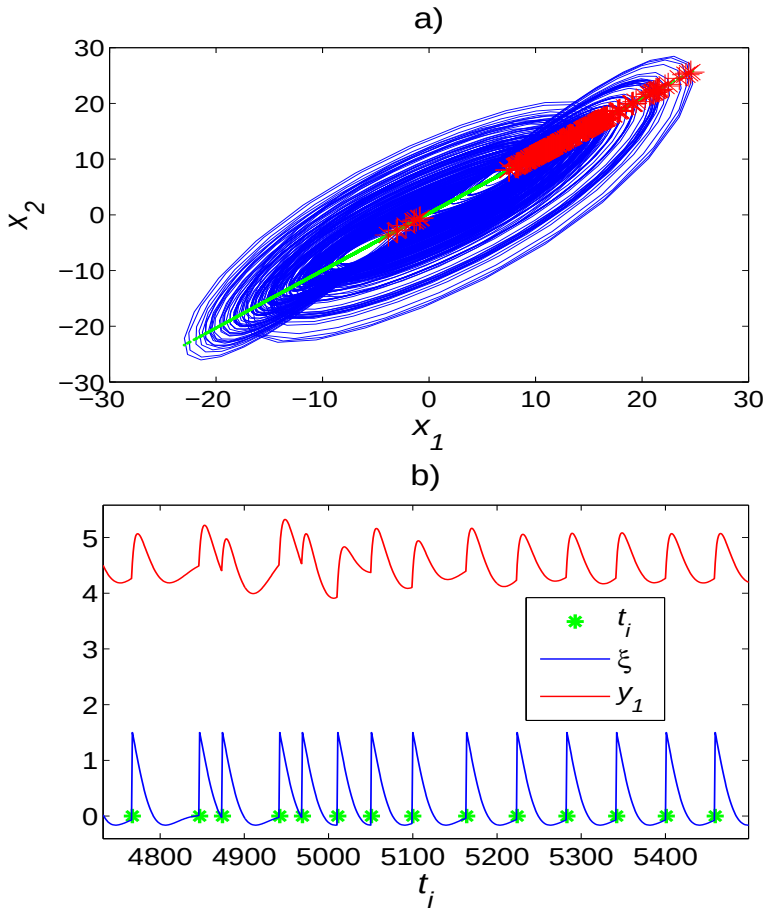

Figure A.10: a) Projection of the monitored Chen system onto the plane (x_1, x_2) intersected by the Poincaré plane Σ. The points of each crossing event $\{\varphi_m^{t_0}(\mathbf{x}_0), \varphi_m^{t_1}(\mathbf{x}_0), \varphi_m^{t_2}(\mathbf{x}_0), \dots\}$ are marked with asterisk. b) Signal $\xi(t)$ from a monitored Chen system marked in solid line, and state y_1 of the forced Lorenz system marked with dashed line. Marked with asterisk the t_i of the crossing events with $A = 1.5, \tau = 0.05$, $\omega = \pi/50$ and $K = 20$.